ARCHIVES OF ELECTRICAL ENGINEERING VOL. 67(1), pp. 139–149 (2018)

DOI 10.24425/118997

New solutions to a multi-objective benchmark problem of induction heating: an application of computational biogeography and evolutionary algorithms

PAOLO DI BARBA[1], FABRIZIO DUGHIERO[2], MICHELE FORZAN[2], MARIA EVELINA MOGNASCHI[1], ELISABETTA SIENI[2]

[1] *Department of Electrical, Computer and Biomedical Engineering*
University of Pavia
Via Ferrata 5, 27100 Pavia, Italy

[2] *Department of Industrial Engineering*
University of Padova
Via Gradenigo 6/A, 35131 Padova, Italy
e-mail: eve.mognaschi@unipv.it

(Received: 03.10.2017, revised: 10.12.2017)

Abstract: In induction heating the design of the inductor implies the solution of coupled electromagnetic and thermal fields, along with the use of optimal design procedures to identify the best possible device or process. The benchmark model proposed, a graphite disk heated by means of induction, is optimized using different optimization algorithms. The design aim requires to achieve a prescribed and uniform temperature distribution in the workpiece maximizing the system efficiency.

Key words: induction heating, multi-physics analysis, multi-objective optimization, benchmark

1. Introduction

Induction heating is generally used for thermal processes of materials [1–3]. In fact it allows a good temperature control of the workpiece temperature with a high efficiency [4–6]. In this field the solution of coupled electromagnetic and thermal problems is mandatory [7–9], as well as the use of optimization algorithms to identify the best device [10–15].

In the paper, the induction heating benchmark proposed in [12–14] is used to test the performances of different multi-objective optimization algorithms. The benchmark model represents an industrial equipment for the epitaxial processing of a silicon wafer [17]. The device to be optimized is an inductor with 12 copper turns and a ferrite yoke that heat a graphite disk [16], as shown in Fig. 1.

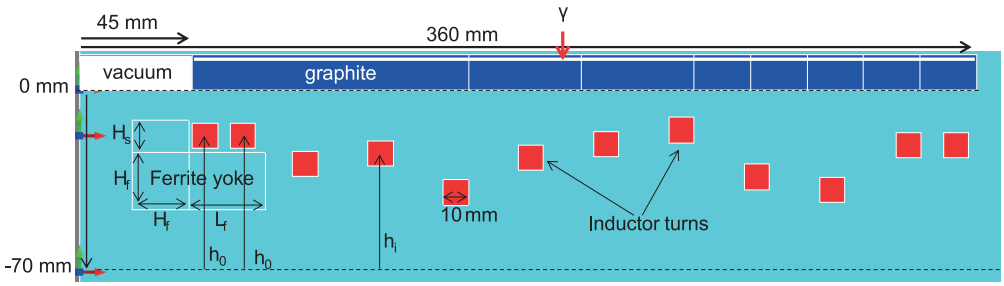

Fig. 1. Geometry and design variables of the induction heating benchmark

The finite-element analysis (FEA) [18] is used to solve the forward problem, whereas the optimization is performed by means of different optimization algorithms: the Non-dominated Sorting Genetic Algorithm NSGA-II [19, 20], Self-Adaptive Migration Non-dominated Sorting Genetic Algorithm SA-MNSGA [21], derived by MNSGA [22], and Biogeography-based Multiobjective Optimization BiMO [23, 24]. The direct problem solves a time-harmonic magnetic problem to evaluate the power density in the graphite disk coupled to a steady-state thermal problem to evaluate the temperature profile [25]. The inverse problem includes 14 design variables: the vertical positions of the turns, the size of a ferrite yoke used to concentrate the magnetic field and the supply voltage. The objective functions are the device efficiency and the temperature uniformity in the workpiece [14] that has to be close to 1150°C at steady state, both objectives are maximized.

2. Forward problem

The 2D benchmark model, sketched in Fig. 1, includes a graphite disk (electrical and thermal properties at 1200°C: $\rho_g = 7.76\ 10^{-6}$ Ωm, $\lambda = 60$ Wm^{-1}K^{-1}) with a radius of 357.5 mm, a pancake inductor with 12 copper turns and a ferrite ring, magnetic field concentrator, under the most internal turns (one or two) that are located at the same height. All turns, series connected, carry a current in the order of hundreds of Ampère at 4,250 Hz. A total power of about 60 kW is prescribed in the device so that the disk reaches a steady state average temperature of 1150°C, as required by the industrial process.

The corresponding inductor current is tuned in each FEA simulation: the FEA solution is updated with a new value of the inductor current (the source of electromagnetic model) when nonlinear material properties are taken into account in the model. Thermal and electrical properties of materials are in Table 1. In Fig. 2, magnetic relative permeability and magnetization curve of the magnetic concentrator are presented. For the sake of simplicity, the electromagnetic properties of the graphite disk are considered to be constant. This choice has been done in order to have a linear forward problem. It is possible to consider non-linear materials e.g. [26, 27], but this would increase the complexity of the forward problem and its cost, while in this paper the main scope is to provide a multi-physics problem solvable in shortest runtime on a standard hardware platform.

Table 1. Electromagnetic and thermal properties of model materials

Element	**Electromagnetic properties**		
Disk	Graphite (at 1200°C)	$\rho_g = 7.76\ 10^{-6}$ Ωm	$\mu_r = 1$
Inductor	Copper	$\rho_c = 1.6\ 10^{-8}$ Ωm	$\mu_r = 1$
Ferrite ring	Ferrite	–	Nonlinear relative permeability (Fig. 2)
	Thermal properties		
Disk	Graphite	$\lambda = 60\ \mathrm{Wm^{-1}K^{-1}}$	

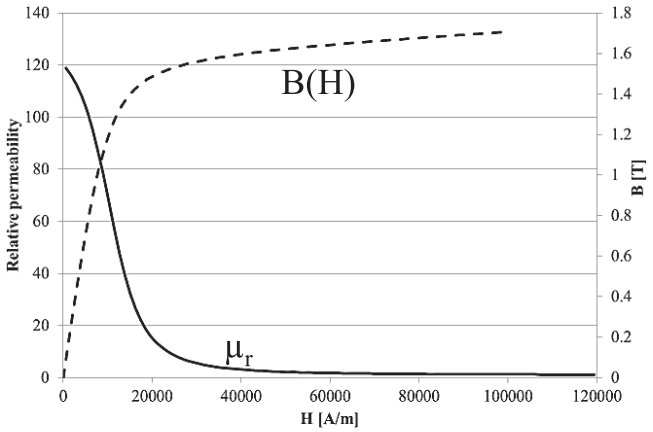

Fig. 2. Relative permeability and magnetization curve of ferrite ring material

The target of the multi-physics design is to evaluate the graphite disk temperature using a given inductor geometry. The magnetic analysis evaluates the power density in the graphite disk starting from the inductor geometry and the supply current. The power density is the source for the thermal problem.

The magnetic problem is solved in time-harmonic conditions by means of a commercial FEA code using the well-known A-V formulation, on second-order elements. The current distribution in each turn is taken into account to correctly evaluate the inductor efficiency. In particular, the magnetic problem is solved in terms of the phasor of the magnetic vector potential, $\boldsymbol{A}$ [18, 28]:

$$\nabla^2 \boldsymbol{A} - j\omega\mu\rho^{-1}\dot{\boldsymbol{A}} = -\mu\dot{\boldsymbol{J}}, \tag{1}$$

where: $\boldsymbol{A}$ and $\boldsymbol{J}$ are the phasors of the current density and magnetic vector potential, respectively, μ is the material magnetic permeability, ρ is the material electrical resistivity and ω is the magnetic field pulsation.

The thermal problem is solved in steady-state condition, assuming the power density in the disk computed by means of the magnetic problem as the source term. The thermal domain is the graphite disk. Along the domain profile a boundary condition of heat exchange along is imposed.

From these assumptions, it results that the solutions of magnetic and thermal problem are weakly coupled by means of the source term of the thermal equation [29]:

$$-\nabla \cdot (\lambda \nabla T) = \rho^{-1} \omega^2 \|\dot{\boldsymbol{A}}\|^2, \tag{2}$$

where λ is the thermal conductivity of the material. Along the disk surface at $r = 0$, and

$$-\lambda \frac{\partial T}{\partial n} = h(T - T_0) + \varepsilon k_B (T^4 - T_0^4), \tag{3}$$

elsewhere, where h is the convective exchange coefficient ($h = 10\ \mathrm{Wm^{-2}K^{-1}}$), ε is the emissivity coefficient ($\varepsilon = 0.6$) and k_B is the Stefan–Boltzmann constant. The external temperature, T_0, is equal to 850°C. These parameters of the thermal model have been tuned in order to fulfill experimental results of a real device as in [17].

A typical second-order mesh to solve the magnetic problem has about 80 000 elements. A zoom of a typical mesh is shown in Fig. 3.

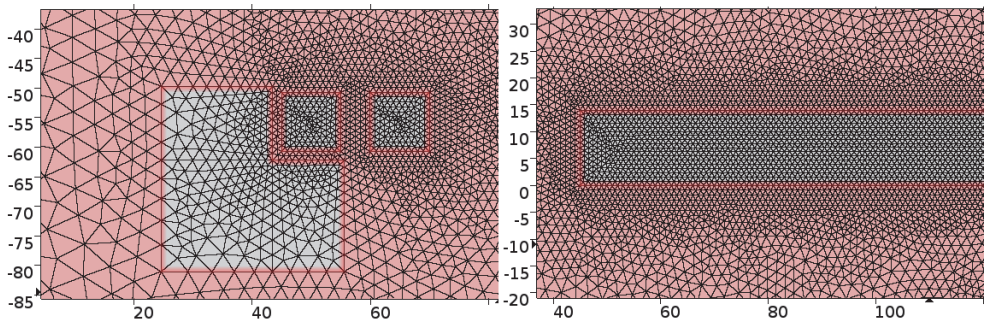

Fig. 3. Mesh detail of ferrite yoke and two turns (left), mesh detail of the disk (right)

Because the thermal domain is the graphite disk only, the disk is the only part of the domain which is meshed for the thermal problem. The temperature has been evaluated on points regularly spaced along the upper line of the disk. A magnetic field map and a temperature field map are shown in Fig. 4.

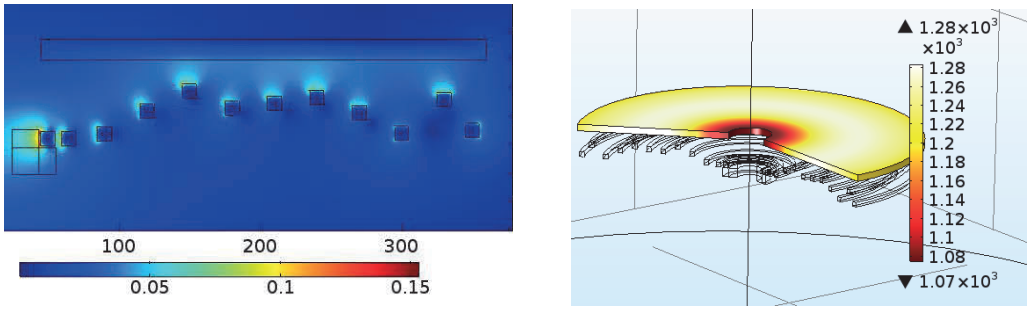

Fig. 4. Magnetic field [T] map (left), temperature [°C] field map (right)

3. Inverse problem

A 14-dimensional vector $\boldsymbol{x}$ of geometric design variables has been defined for the problem; the list of considered design variables with corresponding variation ranges is in Table 2.

Table 2. Design variable ranges

Parameter name	Min	Max	Unit
$h_1,\ldots,h_{10}$	0	60	mm
h_f	10	25	mm
l_f	1	40	mm
V rms	50	600	V

In particular, the design variables are the vertical positions of the inductor turns, the size of the magnetic yoke and the supplied voltage. The design problem is characterized by two conflicting objectives: the maximization of the electrical efficiency, η, defined as the ratio of active power transferred to the disk to the one transferred to the entire device, and maximization of the temperature uniformity along the surface of the graphite disk at thermal steady state. The electrical efficiency, η, is, then, computed from the power density as follows:

$$\eta = \frac{\displaystyle\int_{V_g} \rho_g^{-1}\omega^2\|\dot{\boldsymbol{A}}\|^2\,\mathrm{d}V}{\displaystyle\int_{V_g} \rho_g^{-1}\omega^2\|\dot{\boldsymbol{A}}\|^2\,\mathrm{d}V + \int_{V_c} \rho_c^{-1}\omega^2\|\dot{\boldsymbol{A}}\|^2\,\mathrm{d}V}, \tag{4}$$

where: V_g and V_c are the volume of graphite disk and copper turns, respectively.

In practice, the inverse problem has been implemented as the simultaneously minimization of the following two objective functions:

$$f_1(\boldsymbol{x}) = 1 - \eta(\boldsymbol{x}), \tag{5}$$

$$f_2(\boldsymbol{x}) = \left[1 - \frac{\big(N_j(|T_j(\boldsymbol{x},\gamma) - T_{\text{goal}}| < \text{tol})\big)}{N_{\max}}\right], \tag{6}$$

where: $N_{\max}$ is the number of sampling points, $T_{\text{goal}} = 1150^{\circ}$C is the temperature which should be reached in the disk, and tol = 0.005 i.e. 0.5% is the admitted tolerance.

This way, f_1 is the complementary value of the electrical efficiency and f_2 measures the temperature in-homogeneity in percentage.

In the optimization problem both functions (5) and (6) have to be minimized with respect to design variables shown in Fig. 1 and Table 1: the objective (5) refers to the magnetic domain, while (6) refers to the thermal domain; so, a multi-physics and multi-objective inverse problem is originated. The direct and inverse problems are coupled in order to improve the geometry design of the device in Fig. 1. The multi-physics problem includes the solution in two steps of a magnetic problem and a thermal problem. The magnetic problem step evaluates the efficiency

of the device and the power density, that is the source term of the thermal problem which in turn computes the temperature on the disk surface, related to the second objective function. Electrical efficiency and thermal in-homogeneity are the inputs of the optimization algorithm that generates a new set of design variables vectors.

4. Optimization algorithms

In this paper, the comparison between different algorithms is explored. In particular, a new application of a re-inspired algorithm i.e. biogeography-inspired optimization algorithm (BBO), which was recently extended to the solution of multi-objective inverse problems [22–23], is presented.

On the other hand, in the class of evolutionary algorithms, the recently proposed SA-MNSGA method, which showed good performance when solving optimization problems in electromagnetics, is applied. The main principles behind the two algorithms are now summarized.

Each solution considered in a biogeography-inspired optimization algorithm is treated as a habitat (design vector) composed of suitability index variables (SIV, design variables), and each habitat exhibits a quality given by the habitat suitability index (HSI, objective function) [30]. Remarkably, in contrast to GA-based algorithms, the original population is not discarded after each generation, but it is progressively modified by means of two stochastic operators, i.e. migration and mutation: migration improves the HSI of poor habitats by sharing features from good habitats; in turn, mutation modifies some randomly selected SIV of a few habitats in view of a better exploration of the ecosystem (design space) [31, 32]. In practice, at each generation BBO exploits the HSI of each habitat based on its migration rate, while the emigration rate is set to be complementary to immigration. This way, the HSI of each habitat is improved.

In particular, at each iteration, habitats are sorted from the best ones to the worst ones according to the relevant value of the generalized fitness value. For each SIV of each habitat a random event r_j, such that $0 < r_j < \sup(I,E)$ with I maximum immigration rate and E maximum emigration rate, is generated. Then value r_i is compared with the corresponding immigration rate λ_i of the considered habitat. If $r_j > \lambda_i$ then immigration occurs: the SIV considered in the current ecosystem migrates to the next ecosystem, keeping the same location (Fig. 5).

In contrast, if $r_j < \lambda_i$ emigration occurs: the current SIV in the considered habitat (say the i^{th} habitat) goes extinct and the SIV of another habitat (say the k^{th} habitat) takes the same SIV position in the i^{th} habitat of the next ecosystem. The k^{th} habitat is selected depending on the emigration rate and the SIV.

In the paper, the multiobjective version of the algorithm, already presented by the authors in [33, 34], is applied. It is based on the definition of the generalized fitness, which takes into account simultaneously two or more objective functions by exploiting the concept of non-dominated ranking of solutions in the objective space and crowding distance.

The Self-Adaptive MNSGA, SA-MNSGA, algorithm is a generalized version of the Migration-NSGA, MNSGA, algorithm [21]. Migration strategy applied to the NSGA-II introduces the periodic insertion periodic of a ‘migrated’ population, with a new genetic heritage, in order to modify the genetic heritage of the current population (see Fig. 6).

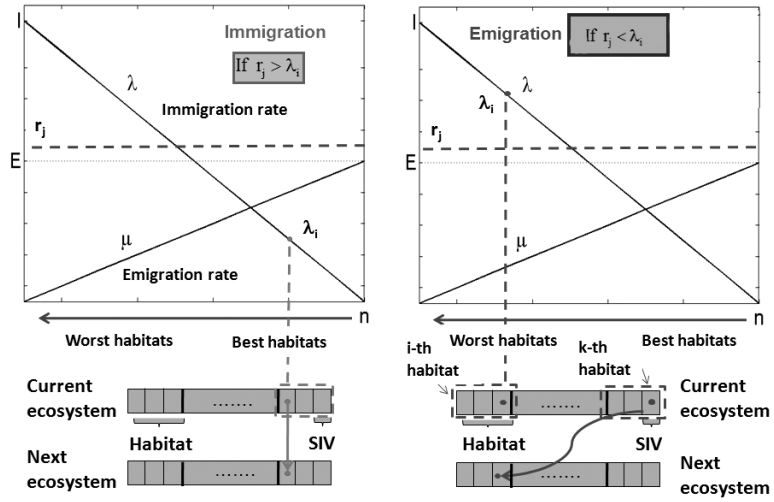

Fig. 5. Schemes of immigration and emigration events

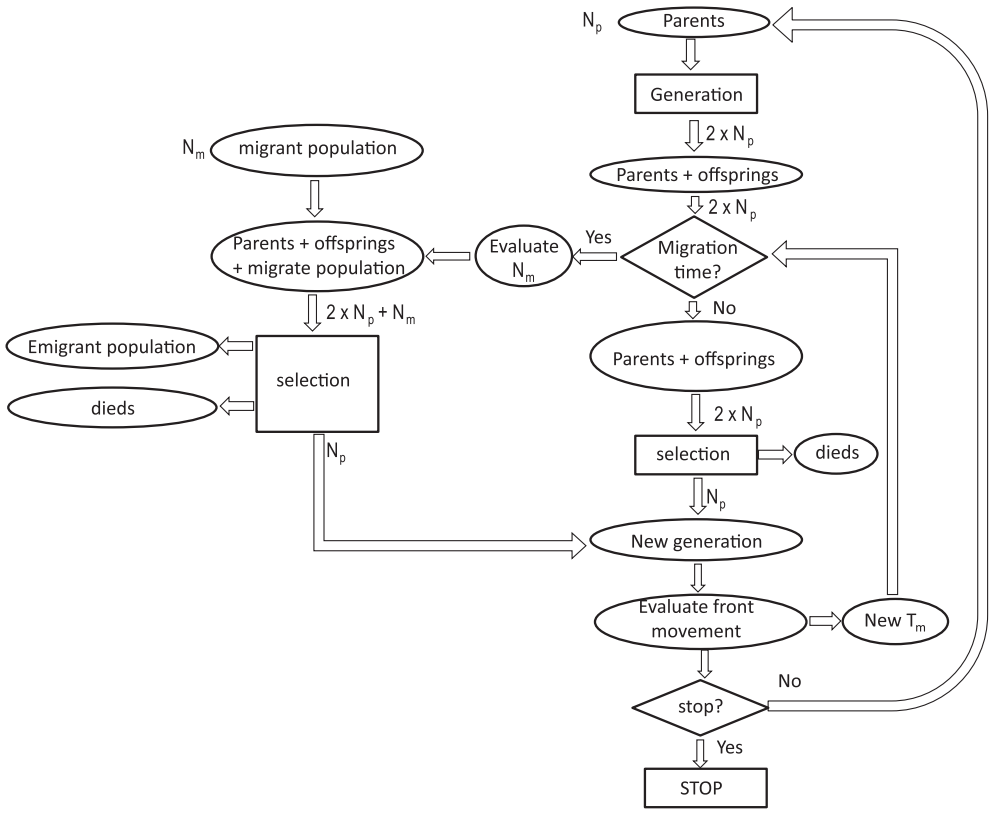

Fig. 6. Flow chart of autiomatic MNSGA algorithm

The first version of MNSGA foresees the periodic migration of a population with a given number of individuals. In the Self-Adaptive MNSGA the occurrence of migration events are based on front mobility. In practice, when the front moves substantially, each migration event introduces a new population with a small number of individuals and the occurrence frequency is low. In contrast, if the front is stable, migration events are more frequent and involve more individuals, up to the size of the initial population (e.g. $N_p = 20$). Migration handling is performed using the strategy described in [21, 22].

5. Results

The three optimization methods are run considering 20 individuals for the population size and 100 generations as stopping criterion. The mutation index for BiMO is set to 0.08, for the NSGA and SA-MNSGA *mum* = 2. The results are shown in Fig. 7.

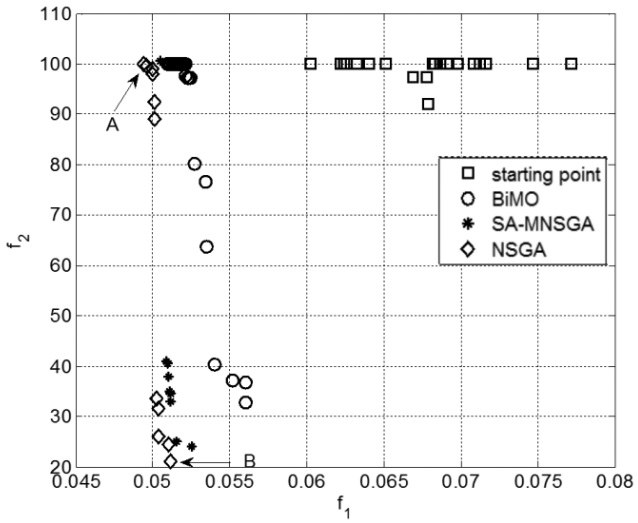

Fig. 7. Optimization results: the starting points and the arrival points for the three optimization algorithms applied are shown

The NSGA is able to find a good approximation of the Pareto front. Also the SA-MNSGA is able to find a good approximation of the front. Both the methods are not able to discover the approximation of the front in the range of about 40–90 for f_2, while the BiMO covered better this part of the front. Two end-point solutions A and B are described in Table 3 and Fig. 8.

Both the two end-points solutions show values of coil heights close to the maximum values. The dimensions of the ferrite yoke of the two solutions are very similar. Moreover, the supplied voltage is almost the same.

Table 3. Design variables and objective function values for the two end-points of the approximated Pareto front identified in Fig. 6

End-point	h_1	h_2	h_3	h_4	h_5	h_6	h_7	h_8
A	59.8	58.4	60.0	60.0	60.0	59.1	58.3	55.5
B	59.4	57.8	45.2	60.0	60.0	56.2	57.1	45.0
	h_9	h_{10}	h_{11}	h_f	l_f	V	f_1	f_2
A	56.5	59.0	58.3	20.1	3.26	235	0.0495	100
B	49.7	59.0	58.0	23.4	2.92	232	0.0511	21

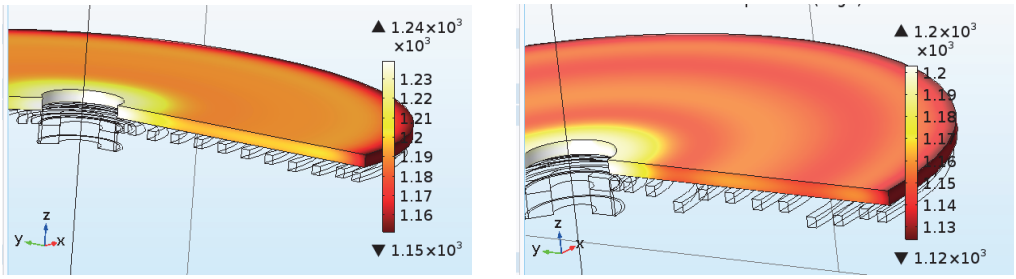

(a) (b)

Fig. 8. Temperature distribution [°C] for the two end-points A (a) and B (b) of the front obtained by NSGA, shown in Fig. 7

6. Conclusions

The three optimization methods applied showed the capability to approximate very well the Pareto front. Each method has its own characteristic which were shown by means of this inverse problem. Hence, this optimization problem, which is multiphysics and multiobjective, is suitable for testing optimization algorithms.

References

[1] Lozinskii M.G., *Industrial applications of induction heating*, Pergamon press (1969).

[2] Barglik J., *Induction heating in technological processes – selected examples of application*, Przegląd Elektrotechniczny, vol. 86, iss. 5, pp. 294–297 (2010).

[3] Mach M., Doležel I., Barglik J., Karban P., *Electromagnetic contactless heat treatment of nonferrous metals and its selected applications*, Proceedings of the 8th International Scientific Conference Electric Power Engineering 2007, EPE 2007, Kouty nad Desnou (Czech Republic), 12–14 June 2007, pp. 110–123 (2007).

[4] Schlesselmann D., Yu Z., Dalinger A., Nacke B., *New applications of numerical simulation in inductive surface hardening with flux concentrators*, HTM – Journal of Heat Treatment and Materials, vol. 70, no. 1, pp. 40–49 (2015).

[5] Baake E., Nacke B., *Efficient heating by electromagnetic sources in metallurgical processes: recent applications and development trends*, Przegląd Elektrotechniczny, vol. 86, no. 7, pp. 11–14 (2010).

[6] Pleshivtseva Y., Zaikina N., Nacke B., Nikanorov A., *Time-optimal control of energy – Efficient heating of aluminium billets rotating in DC magnetic field*, Przegląd Elektrotechniczny, vol. 84, no. 11, pp. 120–123 (2008).

[7] Kotlan V., Karban P., Ulrych B., Doležel I., Kůs P., *Hard-coupled modeling of induction shrink fit of gas-turbine active wheel*, Studies in Computational Intelligence, vol. 483, pp. 325–339 (2013).

[8] Barglik J., Wieczorek T., Smalcerz A., *Modeling of the surface induction hardening process*, Przegląd Elektrotechniczny, vol. 90, no. 2, pp. 1–4 (2014).

[9] Barglik J., Golak S., *Modelling of filling a mold with molten metal in the presence of an electromagnetic field, Magnetohydrodynamics*, vol. 51, no. 1, pp. 5–14 (2015).

[10] Zgraja J., *The optimisation of induction heating system based on multiquadric function approximation*, COMPEL – The International Journal for Computation and Mathematics in Electrical and Electronic Engineering, vol. 24, no. 1, pp. 305–313 (2005).

[11] Mach F., Adam L., Kacerovský J., Karban P., Doležel I., *Evolutionary algorithm-based multi-criteria optimization of triboelectrostatic separator*, Journal of Computational and Applied Mathematics, vol. 270, pp. 134–142 (2014).

[12] Di Barba P., Dughiero F., Forzan M., Sieni E., *Improved solution to a multi-objective benchmark problem of inverse induction heating*, International Journal of Applied Electromagnetics and Mechanics, vol. 49, no. 2, pp. 279–288 (2015).

[13] Di Barba P., Dughiero F., Forzan M., Sieni E., *A Paretian Approach to Optimal Design With Uncertainties: Application in Induction Heating*, IEEE Transactions on Magnetics, vol. 50, pp. 917–920 (2014).

[14] Di Barba P., Forzan M., Sieni E., *Multiobjective design optimization of an induction heating device: A benchmark problem*, International Journal of Applied Electromagnetics and Mechanics, vol. 47, no. 4, pp. 1003–1013 (2015).

[15] Lupi S., Forzan M., Aliferov A., *Induction and direct resistance heating: theory and numerical modelling*, Springer (2015).

[16] Pleshivtseva Y., Di Barba P., Rapoport E., Nacke B., Nikanorov A., Lupi S., Sieni E., Forzan M., *Multi-objective optimisation of induction heaters design based on numerical coupled field analysis*, International Journal of Microstructure and Materials, vol. 9, no. 6, pp. 532–551 (2014).

[17] Forzan M., Maccalli G., Valente G., Crippa D., *Design of an innovative heating process system for the epitaxial growth of silicon carbide layers wafer*, Proc. of MMP – Modelling for Material Proc., (2006).

[18] Binns K.J., Lawrenson P.J., Trowbridge C.W., *The analytical and numerical solution of electric and magnetic fields*, Chichester: Wiley (1992).

[19] Deb K., *Multi-Objective Optimisation Using Evolutionary Algorithms*, Wiley (2001).

[20] Deb K., Pratap A., Agarwal S., Meyarivan T., *A fast and elitist multiobjective genetic algorithm: NSGA-II*, IEEE Transactions on Evolutionary Computation, vol. 6, no. 2, pp. 182–197 (2002).

[21] Bertani R., Forzan M., Sgarbossa P., Sieni E., Di Barba P., Spizzo F., Del Bianco L., *Multi-objective design of a magnetic fluid hyperthermia device*, IECON 2015 – 41st Annual Conference of the IEEE Industrial Electronics Society, no. 7392660, pp. 3603–3608 (2015).

[22] Sieni E., Di Barba P., Forzan M., *Migration NSGA: method to improve a non-elitist searching of Pareto front, with application in magnetics*, Inverse Problems in Science and Engineering IPSE, vol. 24, no. 4, pp. 543–566 (2016).

[23] Di Barba P., Dughiero F., Mognaschi M.E., Savini A., Wiak S., *Biogeography-Inspired Multiobjective Optimization and MEMS Design*, IEEE Transactions on Magnetics, vol. 52, no. 3, pp. 1–4 (2016).

[24] Di Barba P., Mognaschi M.E., Savini A., Wiak S., *Island biogeography as a paradigm for MEMS optimal design*, IJAEM, vol. 51, no. S1, pp. 97–105 (2016).

[25] Di Barba P., Dolezel I., Karban P., Kus P., Mach F., Mognaschi M.E., Savini A., *Multiphysics field analysis and multiobjective design optimization: a benchmark problem*, Inverse Problems in Science and Engineering IPSE, vol. 22, no. 7 (2014).

[26] Zgraja J., Cieslak A., *Induction heating in estimation of thermal properties of conductive materials*, The International Journal for Computation and Mathematics in Eelectrical and Electronic Engineering, vol. 36, iss. 2, pp. 458–468 (2017).

[27] Cieslak A., Zgraja J., *Induction heating laboratory stand for estimating thermal properties of a charge*, Przegląd Elektrotechniczny, vol. 92, iss. 3, pp. 57–60 (2016).

[28] Stratton, J.A., *Electromagnetic Theory*, John Wiley & Sons, Inc., Hoboken, NJ (2007).

[29] Holman, J.P., *Heat Transfer*, McGrawHill, New York, NY (2001).

[30] Simon D., *Biogeography-Based optimization*, IEEE Transactions on Evolutionary Computation, vol. 12, pp. 702–713 (2008).

[31] Singh U., Kumar H., Kamal T.S., *Design of Yagi–Uda Antenna Using Biogeography Based Optimization*, IEEE Transactions on Antennas and Propagation, vol. 58, pp. 3375-3379 (2010).

[32] Dos Santos Coelho L., Alotto P., *Electromagnetic optimization using a cultural self-organizing migrating algorithm approach based on normative knowledge*, IEEE Transactions on Magnetics, vol. 45, pp. 1446–1449 (2009).

[33] Di Barba P., Mognaschi M.E., Venini P., Wiak S., *Biogeography-inspired multiobjective optimization for helping MEMS synthesis*, Archives of Electrical Engineering, vol. 66, no. 3, pp. 607–623 (2017).

[34] Di Barba P., Mognaschi M.E., Krawczyk A., *The biogeography-inspired optimization for the design of coils for nerve stimulation*, 17th IEEE International Conference on Smart Technologies, EUROCON 2017 – Conference Proceedings, 6-8 July 2017, pp. 542–545 (2017).